AIP Advances

RESEARCH ARTICLE | FEBRUARY 11 2026

Quantifying magnetic degradation in laser-cut electrical steel: A domain-level study with angle-dependent magnetization

Special Collection: 70th Annual Conference on Magnetism and Magnetic Materials

Rawal Shahbaz ; Changgeng Zhang ; Hina Fatima ; Hao Zhang ; Yan Zhang

Check for updates

AIP Advances 16, 025124 (2026)
https://doi.org/10.1063/9.0000978

View Online
Export Citation

Articles You May Be Interested In

Two-scale structure of the current layer controlled by meandering motion during steady-state collisionless driven reconnection

Phys. Plasmas (July 2004)

Single particle motion near an X point and separatrix

Phys. Plasmas (June 2004)

11 February 2026 23:33:48

AIP Advances
Why Publish With Us?
19 DAYS average time to 1st decision
500+ VIEWS per article (average)
INCLUSIVE scope
Learn More
AIP Publishing

AIP Publishing

Quantifying magnetic degradation in laser-cut electrical steel: A domain-level study with angle-dependent magnetization

Cite as: AIP Advances 16, 025124 (2026); doi: 10.1063/9.0000978
Submitted: 4 October 2025 • Accepted: 28 November 2025 •
Published Online: 11 February 2026

View Online Export Citation CrossMark

Rawal Shahbaz,[1,2] Changgeng Zhang,[1,2,a)] Hina Fatima,[3] Hao Zhang,[1,2] and Yan Zhang[1,2]

AFFILIATIONS

[1] State Key Laboratory of Smart Power Distribution Equipment and System, Hebei University of Technology, 300130 Tianjin, China
[2] Hebei Key Laboratory of Equipment and Technology Demonstration of Flexible DC Transmission, Hebei University of Technology, 300130 Tianjin, China
[3] Department of Optical Information Science and Technology, School of Physics, Xidian University, Xi'an 710071, China

Note: This paper was presented at the 70th Annual Conference on Magnetism and Magnetic Materials.
[a)] **Author to whom correspondence should be addressed:** changgeng.zhang@hebut.edu.cn

ABSTRACT

Laser cutting is an accurate and popular manufacturing process as it is largely employed in most industries in cutting and shaping materials, including electrical steel parts. Nevertheless, laser cutting in the production of motor cores attracts concern regarding its effects to the materials. The resulting localized thermal effects in the cutting can cause mechanical stresses which can also influence the magnetic properties of the electrical steel. In this study, magnetic domains, and their evolution on the magnetic properties of magnets on the surface of non-oriented silicon steel are explored. The magnetization has been carried out at different angles (0°, 30°, 45°, 60°, 90°) to examine local hysteresis properties by magneto-optic Kerr effect methods. Findings indicate that laser cutting causes variations in domain orientations along the cutting edge, more core losses and reduced magnetic susceptibility. Hysteresis loss was observed at the cutting edge 10% higher in the longitudinal direction than loss in the center sample. The loss experienced around the cutting edge in the transverse directions is also 1.5 times the loss experienced at the center, in which case, this means that the energy loss is significantly large. These results indicate that the cutting edge can undergo various changes in microstructural or stress microstructure, as compared to the sheet of the center.

© 2026 Author(s). All article content, except where otherwise noted, is licensed under a Creative Commons Attribution (CC BY) license (https://creativecommons.org/licenses/by/4.0/). https://doi.org/10.1063/9.0000978

11 February 2026 23:33:48

I. INTRODUCTION

The study of the consequences of laser cutting on non-oriented silicon steel (35WW250) is important because it determines how this cutting can affect the magnetic property and core losses of the electrical machines.[1] Laser cutting creates thermal and mechanical strains that change the microstructure and domain activities that consequently affect core losses and motor effectiveness.[2] Since the a major portion of the world electricity is used by electric motors, minimizing the degradation caused by cutting is important in the high-efficiency design.[3]

The effects of mechanical cutting are well understood but the aftereffects of laser cutting are not so predictable since the localized heating and stress patterns occur. Further microscopic tools like magneto-optical Kerr effect (MOKE) may also be useful as its considerable discrepancies in the magnetic nature of sheet focus and technological laser-cut edges.[4] Nevertheless, the ambiguities complicate the core loss estimation and inhibit optimization of the conditions of laser processing.[5]

The aim of the systematic review is to generate the existing knowledge on the laser cutting effects of non-oriented silicon steel with emphasis on MOKE-based magnetic property, core loss changes, and comparison of sheet center and laser cutting edge samples.[6,7] This methodology would involve a comprehensive review of experimental studies on the impacts of laser cutting on silicon steel with use of local microscopic measurements.[8] Results

© Author(s) 2026

include changes in magnetic properties, core loss mechanisms and the useful data about domain structure changes under the influence of different angular field excitation.[8,9]

II. METHODOLOGY AND MATERIAL

High-resolution MOKE microscope was used to measure and estimate local hysteresis loops and domain averaged anisotropy in longitudinal and transverse geometries as shown in Fig. 1. A 100 × oil-immersion objective lens was used to properly focus (p-polarized red, 635 nm, and blue, 405 nm) light (53° angle of incidence) onto the sample. An electronically rotating electromagnet having frequency of 10 Hz with recordings taken at every 15° gave an in-plane sinusoidal field $\mu_0 \boldsymbol{H}_{\max} \approx 100$ mT (80 kA m^{-1}). **S** = (**I, Q, U, V**) was reconstructed under a 4-state approach at 200 kS s^{-1} lock-in sampling; Kerr rotation η_k and ellipticity ε_k was found using

$$\varepsilon_K = \frac{1}{2}\arctan(U/Q), \eta_K = 1/2 \arctan\ (V/Q). \quad (1)$$

The longitudinal Kerr constant KL = 0.58° of Fe-3.2 wt. % Si at 635 nm was used to transform the magneto-optic signal to surface magnetization ***M*** after subtraction of background that was measured on the saturated sample. The true internal field was obtained by

$$H_{int} = H_{surf} - NM - H_{demag}. \quad (2)$$

A mixed-field correction that took the 0.35 mm of sheet thickness into account, as well as the 1 mm lift-off by the Hall sensor. For local 8 × 8 μm^2 probed area, N = demagnetizing factor = 0.93 × 10^{-2} (SI).

All of the measurements were carried out on 35WW250 non-oriented Si-steel (thickness 0.35 mm, nominal loss 2.50 W kg^{-1} at

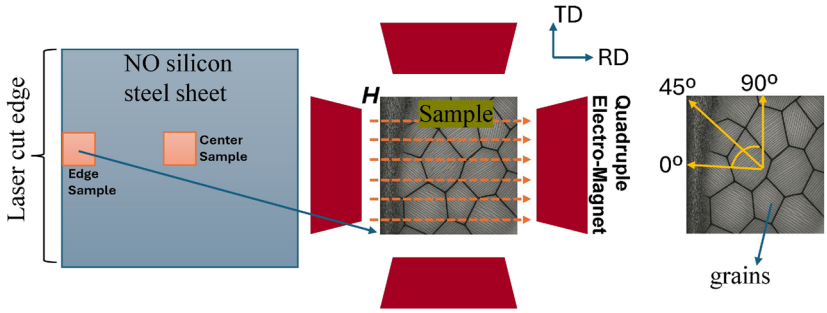


FIG. 1. Experimental setup for MOKE analysis of non-oriented silicon steel, highlighting center and edge samples with domain structures under polarized light.

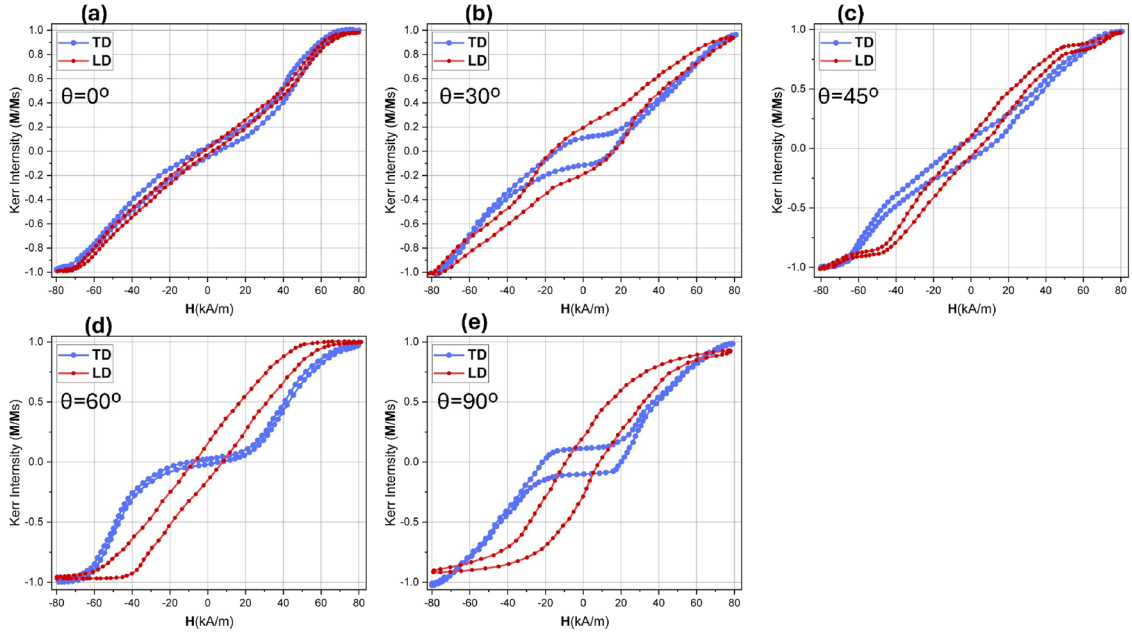


FIG. 2. Magnetization curves along the longitudinal (LD) and transverse direction (TD) at an external field of (0, 30, 45, 60, 90) degree angles from (a)–(e) at the center of sample.

11 February 2026 23:33:48

© Author(s) 2026

1.5 T, 50 Hz).[10] Two 12 × 12 mm^2 samples have been spark-cut one on the center of the sheet, and another one on its nearest edge, industrial laser-cut border (1.5 kW fiber laser, 200 mm s^{-1}, 0.2 mm kerf).

III. RESULTS

The hysteresis loops, sheet center (Fig. 2) indicate a soft magnetic response where it is easily magnetized along the longitudinal direction (LD) indicated by a smaller loop with increased remanence at θ = 30°, 90°. With increasing field angle, the LD loop, transverse direction (TD) loop increases in width signifying decreased anisotropy and increased reversible magnetization.

In sharp contrast, loops closer to the laser-cut edge (Fig. 3) are much broader and have a more magnetic epitome, as well as much greater coercivity. Coercivity increases at intermediate angles (30°, 45°), it slightly decreases at 90°, possibly due to the saturation alignment of magnetization parallel to the applied field and partial domain wall relaxation.

Coercivity $\boldsymbol{H}_c$ and remanence $\boldsymbol{M}_r$ were extracted from the $d\mathbf{M}/d\mathbf{H}_{int}$ peak and the zero-crossing of $\boldsymbol{H}_{int}$, respectively that is presented in Figs. 4(a) and 4(b). From Eq. (3)

$$H_c^{edge} = H_c^{center}\left[1 + \eta_H \sqrt{N_d^{HAZ}}\right]. \tag{3}$$

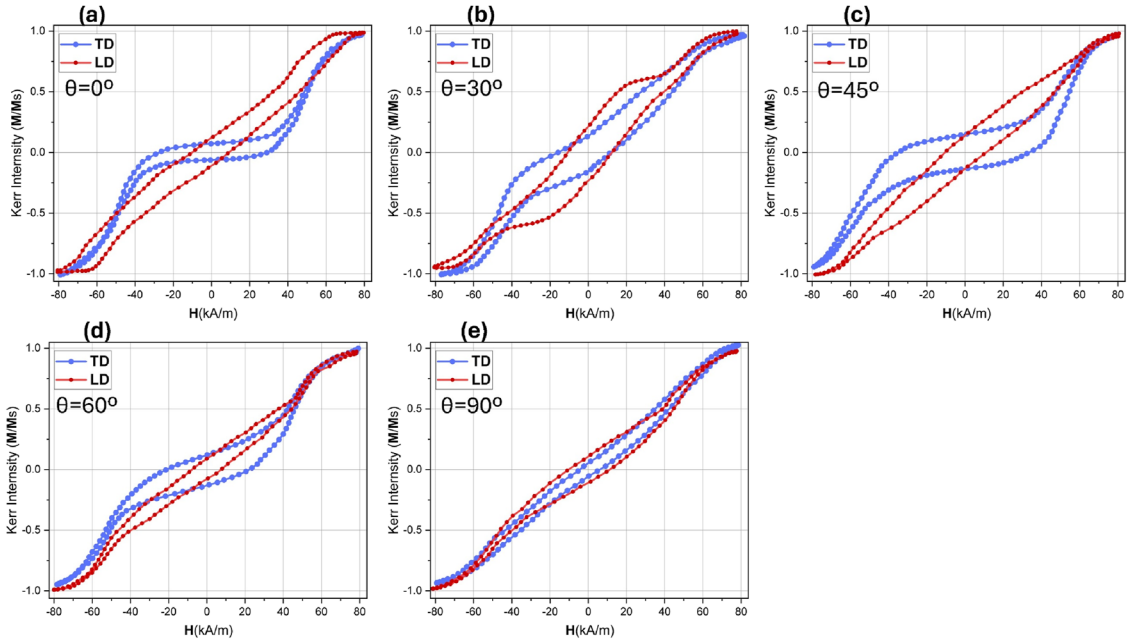


FIG. 3. Magnetization curves along the longitudinal (LD) and transverse (TD) directions at an external field of (0, 30, 45, 60, 90) degrees from (a)–(e) near the cutting edge.

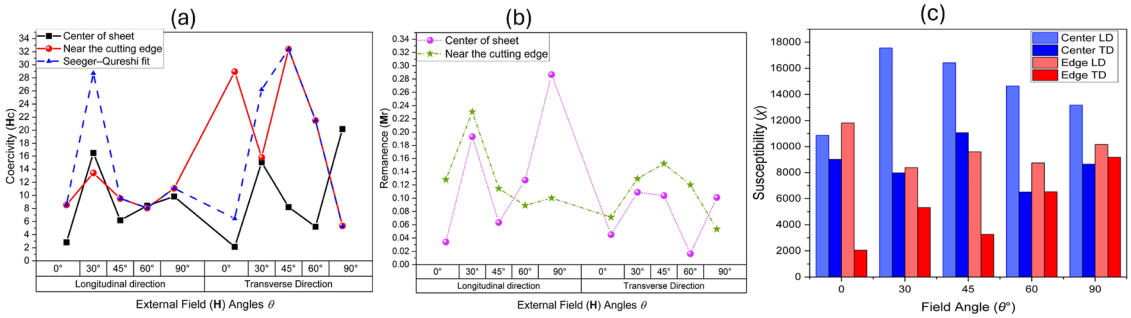


FIG. 4. (a) Coercivity exhibits angular dependence with a peak between 30°–45°, slightly reducing at 90°, consistent with partial relaxation of domain wall pinning; dashed line: from Eq. (3) with $k(\theta) = 2.03 + 1.94\cos(2\theta) + 0.35\cos(4\theta)$ fitted to the data. (b) Remanence (M_r) values and (c) Magnetic susceptibility (χ) in the low-field region (20 kA/m) as a function of (H) angle (θ).

11 February 2026 23:33:48

© Author(s) 2026

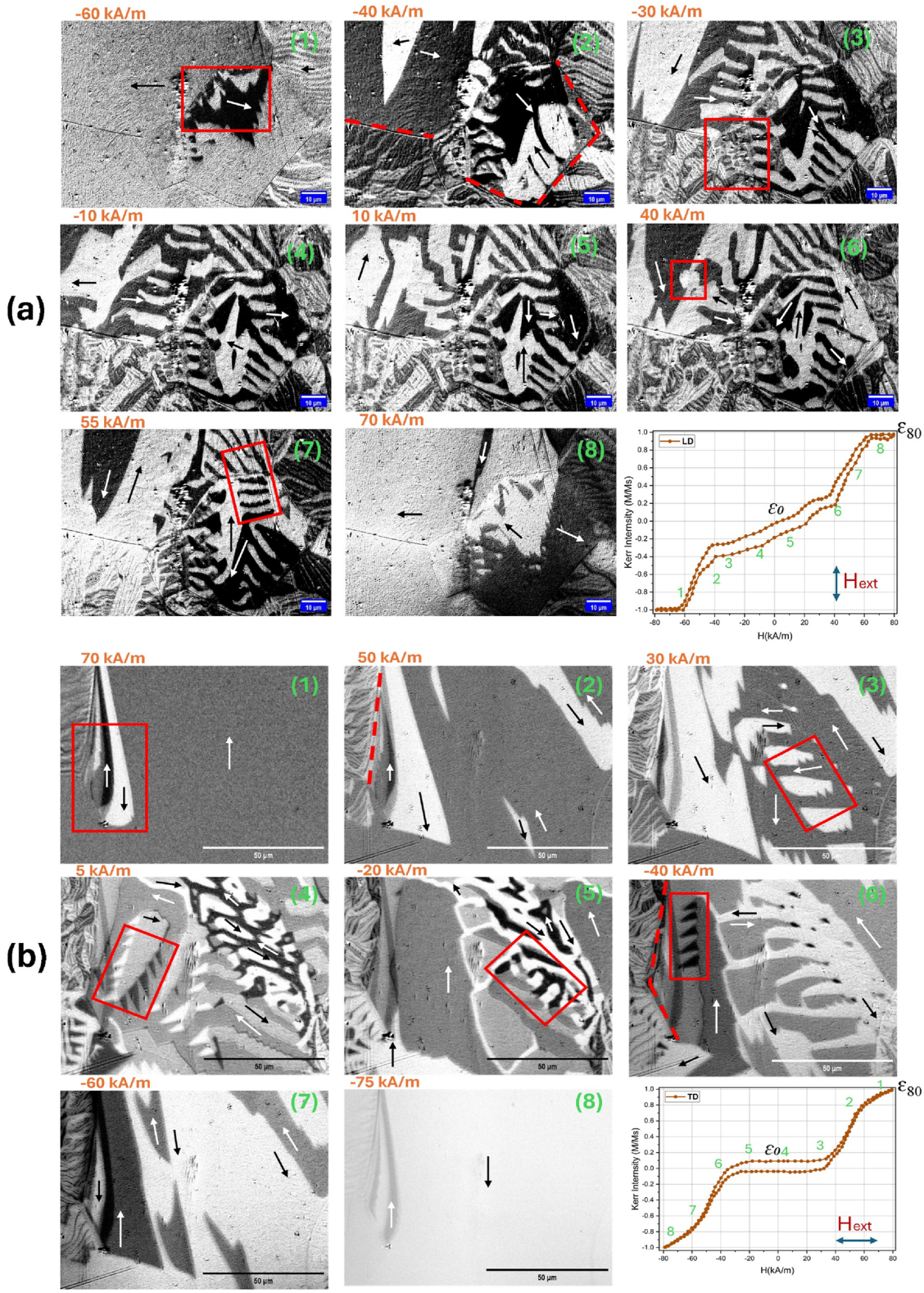


FIG. 5. Domain pattern corresponding to the green points mentioned in the hysteresis curve taken with (a) longitudinal, (b) transverse MOKE near the cutting edge.

11 February 2026 23:33:48

© Author(s) 2026

The coercivity measured by MOKE 50 μm from the cut edge is higher than in the sheet center because the Heat-Affected-Zone (HAZ) contains extra dislocations (N_d^{HAZ}) that pin domain walls. The angular dependence of the additional coercivity is in a shape of a 2-fold-cosine with maximum enhancement ≈ 2.0 kA m^{-1} along θ = 0° and 45°, which are consistent with the Seeger-Qureshi square-root law observed in Ref. 11. η_H is the same proportionality constant that is already calibrated for DC04 steel in Ref. 12.

After subtracting the internal-field error the actual hysteresis loss W_h:

$$W_h = \oint \mu_0 \boldsymbol{H}_{int} d\boldsymbol{M}. \tag{4}$$

At center position with $\theta = 0^\circ$ at 1 mm below the laser cut edge, integration provides $\boldsymbol{W_h}$ = 2.18 ×10^{-2} J kg^{-1}; at 2.4 mm below the laser cut edge with the same angle, the sample provides 2.40 × 10^{-2} J kg^{-1} a 10% increase. The higher loss at 2 mm due to the edge effect probably results from the existence of a transition region in which domain wall bowing through the localized annulment of hysteresis is still occurring but the defects remain to cause a small increase in loss before it flattens off at the center. The greatest difference becomes in the transverse $\theta = 90^\circ$ direction where the edge value of 3.35 × 10^{-2} J kg^{-1} is 1.5 times the center position of 2.23 × 10^{-2} J kg^{-1} which is previously predicted.

In Fig. 4(c), low field (20 kA/m) magnetic susceptibility (χ) was given which is inversely related to coercivity. The Center LD is the most easily magnetized with the peak of this frequency taken up by practically 18 000 at 30°. The "Edge TD" in comparison has greatly lower susceptibility to the order of less than 5500 and falls to about 3200 at 45°.

IV. DISCUSSION

Domain images also had been obtained of the center region, but owing to the restrictions on figures to be used there are given only representative edge-domain images. The center domains displayed regular strip structures with the least amount of variation and which acts as a reference point of comparison.

Some red squares are highlighted in Fig. 5(a), first image represents domain nucleation and the other shows different domain pinning sites and grain boundary domains at 55 kA/m, strips type domain appear but at 90° position. Stresses due to cutting, create energy wells which can be observed in TD domains at point (3–6) in the red square box some domains are triangular shape that represents pin domain walls and the red dotted lines are showing grain boundaries. It needs more external field to overcome such energy barriers and hence rises coercivity. We evaluate the local effective field from

$$H_{eff} = H_{ext} - \nabla \cdot H_d + H_{ani} \tag{5}$$

using quantities extracted in Sec. III. $\boldsymbol{H}_{ext}$ = 80 kA m^{-1} at the point of the loop when $\theta = 0^\circ$. The Hall-map directly provides a demagnetizing gradient $\nabla \cdot \boldsymbol{H}_d$ = −0.7 kA m^{-1} within the 50 μm-calner heat-affected region, and the angle resolved fit anisotropy provides $\boldsymbol{H}_{\text{ani}}$ = 0.37 kA m^{-1} at the center and 0.51 kA m^{-1} at the edge. Equation (5) therefore yields center: $\boldsymbol{H}_{eff}$ ≈ 81.1 kA m^{-1}, edge: $\boldsymbol{H}_{eff}$ ≈ 81.2 kA m^{-1}. The 0.1 kA m^{-1} extra field at the edge is only enhanced at the center by 0.12%, and the 38% coercivity gain. The ratio of $\frac{\varepsilon_0}{\varepsilon_{80}}$ the squareness of the loop is clearly less in the transverse direction (e.g., = 0.114 at TD) than in the longitudinal direction (e.g., = 0.740 at LD), indicating a lesser level of magnetic response.

V. CONCLUSION

In angle-resolved Kerr microscopic studies, industrial laser cutting increases local coercivity by 40%, and hysteresis loss by 10% along the rolling direction at 1mm off the edge, and transverse losses are 1.5 times greater than those of near cutting edge compared to center sample of sheet. Domain images all show weaker with branch strips that ascertain the fact that tensile stresses generated by the cutting enhance the basic stripe geometry of the material. When these occur in the cutting, motor-design programs may need to adopt the position-dependent and angle-dependent loss data for degenerate silicon steel.

ACKNOWLEDGMENTS

This work was supported by the National Natural Science Foundation of China, (No. 52277008, 52130710), and Natural Science Foundation of Hebei Province, China (No. E2023202050, E2024202298).

AUTHOR DECLARATIONS

Conflict of Interest

The authors have no conflicts to disclose.

Author Contributions

Rawal Shahbaz: Investigation (equal); Methodology (equal); Writing – original draft (equal). **Changgeng Zhang**: Conceptualization (equal); Supervision (equal); Writing – review & editing (equal). **Hina Fatima**: Methodology (equal); Software (equal); Writing – review & editing (equal). **Hao Zhang**: Methodology (supporting). **Yan Zhang**: Resources (supporting).

DATA AVAILABILITY

The data that support the findings of this study are available from the corresponding author upon reasonable request.

REFERENCES

[1] C. Zhang, Y. Zhang, Y. Li, and Q. Yang, "Magnetic properties deterioration of non-oriented steel due to laser cutting," AIP Adv. **13**(2), 025360 (2023).
[2] M. Alsaadawy, M. Dewidar, A. Said, I. Maher, and T. A. Shehabeldeen, "A comprehensive review of studying the influence of laser cutting parameters on surface and kerf quality of metals," Int. J. Adv. Manuf. Technol. **130**(3–4), 1039 (2024).
[3] N. Alatawneh, A. Saleem, T. Rahman, D. A. Lowther, and R. Chromik, "Modelling and analysis of the effects of cutting of core laminations in electric machines," IET Electr. Power Appl. **14**(12), 2355 (2020).
[4] C. Backes, M. Kahlert, M. Vollmer, M. Smaga, T. Niendorf, and T. Beck, "Microstructure and magnetic domain structure of additively manufactured Fe–Si soft magnetic alloys with 3 and 9 wt.-% Si," J. Mater. Res. Technol. **29**, 1691–1702 (2024).

11 February 2026 23:33:48

© Author(s) 2026

[5]Ş. Bayraktar and Y. Turgut, "Experimental and statistical analysis of the effects of punching and laser cutting methods on induction motor efficiency and total magnetic losses in silicon lamination sheets," J. Magn. Magn. Mater. **572**, 170599 (2023).
[6]M. Dems, K. Komeza, Z. Gmyrek, and J. Szulakowski, "The effect of sample's dimension and cutting technology on magnetization and specific iron losses of FeSi laminations," Energies **15**(6), 2086 (2022).
[7]C. Zhang, L. Yang, and Y. Li, "Punching effects on local magnetic properties near the edge of nonoriented electrical steels," COMPEL - Int. J. Comput. Math. Electr. Electron. Eng. **42**(1), 159–168 (2023).
[8]S. Elfgen, P. Rasilo, and K. Hameyer, "Hysteresis and eddy-current losses in electrical steel utilising edge degradation due to cutting effects," Int. J. Numer. Modell.: Electron. Networks, Devices Fields **33**, e2781 (2020).
[9]A. Gottwalt-Baruth, P. Kubaschinski, M. Waltz, and U. Tetzlaff, "Influence of the cutting method on the fatigue life and crack initiation of non-oriented electrical steel sheets," Int. J. Fatigue **180**, 108073 (2024).
[10]K. Winter, Z. Liao, E. Abbá, J. R. Linares, and D. Axinte, "Effect of sub-micron deformations at opposing strain rates on the micromagnetic behaviour of non-oriented electrical steel," Nat. Commun. **15**, 9010 (2024).
[11]M. Domenjoud and L. Daniel, "Effects of plastic strain and reloading stress on the magneto-mechanical behavior of electrical steels: Experiments and modeling," Mech. Mater. **176**, 104510 (2023).
[12]B. Ducharne, S. Zurek, L. Daniel, and G. Sebald, "An anisotropic vector hysteresis model of ferromagnetic behavior under alternating and rotational magnetic field," J. Magn. Magn. Mater. **549**, 169045 (2022).

11 February 2026 23:33:48

© Author(s) 2026